Int J Clin Exp Med 2021;14(2):840-851
www.ijcem.com /ISSN:1940-5901/IJCEM0118674

Original Article

MRI diagnosis of the knee, bone inflammation, and disease evaluation

Xia Zhang[1], Yunbo Bai[2], Weiguang Song[2], Xiaowen Liu[3], Xiaochun Tang[1], Qingxue Meng[1], Guangbin Wang[1]

[1]Department of Medical Imaging, Yiyuan People's Hospital, Zibo, China; [2]Department of Orthopedics,Yiyuan People's Hospital, Zibo, China; [3]Ultrasonography Room of Shandong Institute of Endocrine & Metabolic Diseases, Shandong First Medical University & Shandong Academy of Medical Sciences, Jinan, China

Received July 22, 2020; Accepted October 28, 2020; Epub February 15, 2021; Published February 28, 2021

Abstract: Objective: This study examines chronic joint disease, joint swelling and deformation, joint pain, and joint nonunion caused by knee femur osteoarthritis, which seriously affect patients' lives and health. The purpose of this study was to investigate the correlation among the MRI morphological scores, the T_2 values, and the clinical manifestations of cartilage injuries in knee osteoarthritis. Methods: SPSS 19.0 statistical software was used for the data analysis. The measured data are expressed as the mean ± standard deviation. All the tests are double sided. The reliability was 95%, and the significance level was 0.05. Chi square tests and t-tests were used to compare the general data of the OA and control groups, and Pearson simple correlation analyses were used to evaluate the correlations between the T_2 values of the cartilage in each subregion of the OA group and the WORMS. Results: The analysis found that the OA group had skeletal areas, medial femur areas, medial tibial areas, and the correlation coefficients between the cartilage T_2 values and the WORMS in the lateral tibia were 0.66, 0.72, 0.71, and 0.85 ($P < 0.05$). The T_2 value in the lateral femurs and the WORMS correlation coefficient was -0.03 ($P > 0.05$). The T_2 value of each sub-region gradually increased with the increase of the grade. The results show that, except for the T_2 value between the H group and the 01 group in the lateral region of the tibia, there was no significant difference in the T_2 value between the 01 group and the 02 group in the skeletal region ($P < 0.05$), and the differences in the other subregions were statistically significant between the groups. The T_2 value of the best test performance of the bone region between the H group and the 01 group was 34.25 ms using the Jordon index, the most approximate index was 0.87, the sensitivity was 78.23%, the specificity was 100%, and the area under the curve was 0.82. The best T_2 test performance of the medial femoral region between the H and 01 groups was 45.21, the most approximate index was 0.47, the sensitivity was 67.38%, the specificity was 79%, and the area under the curve was 0.76. The medial tibia of the best test performance between the H group and the 01 group was 32.48 ms, the most approximate index was 0.38, the sensitivity was 44.73%, the specificity was 69%, and the area under the curve was 0.52. Conclusion: This method can accurately diagnose knee joint arthritis, enabling the prompt control of the disease progression and effectively reducing the disability and mortality rates the disease causes, thus improving patients' quality of life.

Keywords: Magnetic resonance imaging, T_2 pictures, knee osteitis, osteoarthritis, articular cartilage

Introduction

At present, the commonly used imaging methods in clinical practice include X-rays, computed tomography (CT), magnetic resonance imaging (MRI), ultrasound, and radionuclide bone imaging [1]. Among them, X-rays are still the primary method for diagnosing skeletal inflammation. X-rays enable the observation of structural changes in bones and the overall morphological changes in multiple joints or their parts at the same time. X-rays have a high spatial resolution and can be used for grades III and IV. Grade skeletal arthritis enables a positive diagnosis, and the examination method is simple and inexpensive, and the patient receives little radiation [2], and X-rays can effectively display the skeletal joint space, small articular cartilage bone plate lesions, osteoporosis, and osteosclerosis around the joint, etc., so it is convenient for measuring the skeletal joint space [3-5].

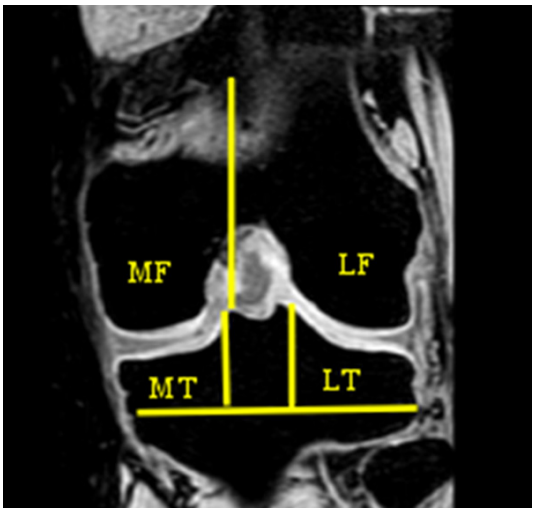

Figure 1. Schematic diagram of the knee cartilage division. The femur is divided into the medial (MF) and lateral (LF) subregions by passing through the medial side of the medial scatter of the femur, where the trochlear groove belongs to the lateral region; the tibia is divided into the medial (MT) based on the medial boundary of the interstitial spine of the tibia and the lateral subarea (LT), the area is 2 cm below the cartilage.

At the same time, MRI also has the advantages of being non-invasive, radiation-free, multi-planar imaging, etc. As the preferred method for the early diagnosis of bone inflammation, judging the disease activity, evaluating the curative effect and judging the prognosis, the ASAS diagnostic criteria for axial bone inflammation in 2009 introduced MRI to improve the specificity and sensitivity of the early diagnosis of bone inflammation [6, 7]. The technology can find arthritis, synovitis, endomyositis, cartilage and bone damage in the detection of bone inflammation, peripheral joint disease, and attachment point inflammation. It employs a quantitative evaluation of arthritis using grayscale values and power Doppler ultrasound. It has become a useful tool for the clinical diagnosis and evaluation of the curative effects, but ultrasound cannot detect axillary attachment point inflammation [7]. It is not advisable to use inflammation to replace the inflammation of the axial skeletal joint and spine. Radionuclide imaging is a concentration of a radionuclide (or its compound) inside or outside the organ, or between the normal and the diseased tissue. It is a poor method for imaging. When bone lesions occur, the local blood flow is increased, osteoblasts are active and new bone is formed, ion exchange and chemical adsorption are enhanced at the local lesions, which are multiple, irregular, and most often appear on bone imaging [8]. The concentrations of bone imaging agents appear in various sizes and shapes. Radionuclide bone imaging has been reported in the early diagnosis of bone inflammation. Radionuclide bone imaging is a quantitative reflection of the skeletal articular bone [9]. The method of mass metabolism can show the changes in bone metabolism at an early stage, indicating the existence of active inflammation. Bone inflammation can involve multiple sites and multiple joints, and, combined with whole body bone imaging, it will be of great value in clarifying the scope of the disease. The sensitivity and specificity of imaging in the diagnosis of skeletal inflammation are lower than MRI, which limits its routine application in clinical practice [10]. In summary, X-rays are still commonly used in clinical practice. MRI, in the diagnosis and assessment of bone inflammation, is an essential tool for determining the early diagnosis of bone inflammation and disease activity, and for prognosis and evaluation, its efficacy is superior to other types of imaging.

Materials and methods

Principles of magnetic resonance imaging

Magnetic resonance imaging (MRI) has been widely applied to biology and medicine since its discovery [5]. It can study the dynamic processes of metabolic changes at the molecular level, calculate the constant rates, quantify the metabolites, and in the process will not affect the organism's activity, maintaining the organism in a normal physiological state. Compared with the previous diagnostic methods, it has evident advantages. It has been widely used in the clinical diagnosis of various diseases. The clinical applications of MRI in the diagnosis of skeletal muscle injuries include T1 weighted imaging (T1WI) and T2 weighted imaging (T2WI). In recent years, some new magnetic resonance techniques have been increasingly applied to skeletal muscle injury experiments, including magnetic resonance diffusion weighted imaging (DWI), magnetic resonance diffusion tensor imaging (DTI), and magnetic resonance spectroscopy (MRS) [11]. **Figure 1** shows the schematic of magnetic resonance imaging.

The biological basis of diffusion tensor imaging

Dispersion is a movement phenomenon caused by the Brownian activity of molecules. In distilled water or solutions, molecular weight, heat, and viscosity among molecules interfere with the dispersion of molecules. The dispersion of water in an organism is also disturbed by various structures or protective membranes in the biological tissues, including various membranes and compartments in the organism (such as various types of extracellular and intracellular morphologies, nerves, and glia) in the body. This interference becomes more and more significant as the dispersion distance increases [12]. It is thought that the existence of the above various interference factors and the dispersion of water molecules in different biological tissues are also different and that water molecules depend on directionality to diffuse [13]. For clear carriers, such as distilled water or an ultrafine morphology, the arranged specimens have the same level of dispersion in each orientation, which is called isotropic dispersion, and for chaotic carriers, and in areas with different directions (such as white matter, skeletal muscle), water flows in all directions. The dispersion perpendicular to the fine form is the hottest, and the dispersion parallel to the fine form is the largest. This is called anisotropic dispersion. DTI is based on this ultra-microscopic activity of water and involves the examination of ultra-morphological and pathological changes of organisms to a certain extent [14].

Diffusion tensor imaging

We generally use tensors to represent the degree of diffusion of the water molecules in an organism. At present, DTI research can be classified into two major directions. The first is quantitative inquiry. DTI evaluates the average dispersion (MD), the tensor trace (Tr) of all the dispersion phenomena, and the anisotropy scores (FA), scalar relative anisotropy (sR A), and volume ratios (VR) and so on to quantify the diffusion tensor. The second research direction studies the shape of water molecules in the tissue, which is detected using fiber bundle tracking technology (FT) [14].

Diffusion tensor imaging technology

The current DTI imaging technology still faces many problems. In the process of DTI imaging, the most essential problem is that it must be sensitive to small activities without being disturbed by large movements. To obtain a diffusion-weighted contrast, diffusion-weighted imaging is sensitive to micron-level molecular activities. We are keen to the big organizational events. Even a small movement (sub-millimeter level) of the subject during the diffusion coding process can cause a small phase change in the acquired echo signal. Since this level of collective activity may be different during the one echo call, the echoes from the two calls may also differ [15]. The second problem encountered in DT imaging is the signal-to-noise ratio and the discrimination rate. Too small a signal-to-noise ratio can transmit errors to each element of the tensor, causing the final value to be inconsistent with the actual value. When the discrimination value is too small, some volume phenomena appear particularly serious, many distortions and many factors are generated in the same individual voxel block, and each has different divergence directions and sizes, so that the voxels will no longer show a single exponential weakening. In addition, the magnetic susceptibility phenomenon, the coding scheme, and the eddy current phenomenon are all problems that DTI must overcome. These two major problems are the most urgent ones that need to be solved by DT industrial imaging and that must be solved by continuously advancing the DT industrial sequence [16].

Imaging sequences

Many DT imaging sequences and techniques have appeared so far. They are all produced by implanting Stejskal-Tanner dispersion-sensitive gradients into other basic sequences. The most commonly-used sequences are: single-shot DT imaging technology, and the most important problem for diffusion weighting is knowing how to reduce or delete the interference of large movements (including inactive activities such as pulse, heartbeat, active activities, such as head rigidity, etc.) on the signal because of diffusion weighting [16]. For the body's activities, determining whether they are major or subtle activities is crucial. The one-time trigger technology can collect a graphic at the sub-second level, so it can completely ignore the body's large activities. In order to obtain all the K-space lines of all the graphics in a single shot EP work sequence, only one RF pulse is needed. Therefore, only one RF pulse is needed to re-

create a graphic, and the total collection time should be at least 100 ms. Most of the big events can be ignored in such a small period of time. This sequence is now used in most DT imaging. It has a dispersion-sensitive completion method similar to the previous sequence, that is, a dispersion-sensitive gradient region with no less than 6 azimuths placed at both ends of the 1800 gathering pulse, and the EPI signal acquisition method is used [17].

Although the single shot EPI sequence ignores the benefits of various activities and the short time required for imaging, it still has some unsolved problems. First, the susceptibility artifacts of the EPI sequence are particularly powerful. Since the phase of the gradient encoding in the EPI collection form does not return to zero and the next phase encoding is started, the second phase encoding will be affected by the phase shift caused by the previous tissue susceptibility, and the echo chain is particularly long. The phase difference has been accumulated, and finally a major graphic twist appears in the phase encoding direction. This kind of artifact is very serious in the brainstem, prefrontal lobe, and other places because the tissue magnetic susceptibility changes in these areas are very obvious [18]. The most severe problem with this technology is the magnetic susceptibility artifact. Eddy current is the second major problem affecting this technology. Eddy currents are caused by the acceleration of the gradient field within the EP sequence. The linearity of the encoding gradient field in space is reduced, so that the encoding mismatch in the space is caused by the eddy current that accumulates in the ordinary gradient current. Now, due to the advances in the previous technology and the emergence of new equipment [19], the eddy current interference has become very small. Low spatial discrimination and signal-to-noise ratios are the third major problems that this technology needs to solve. The injective EPI sequence must collect all the information necessary for a graphic in TR time, but the time required for the organization to weaken T_2 * is particularly short. These two factors have caused the echo chain (when the echo chain time is too long, it will cause the T_2 * phenomenon and the magnetic susceptibility to increase) work to take too long, so the matrix commonly used in clinical and research is 64-128; Also, the EPI sequence is compared with the ordinary spin echo sequence, and the tissue signal is weakened according to T_2 * This determines that under the same TR and TE times, the graphic signal-to-noise ratio is smaller than it is with the ordinary spin echo sequences. There are other deficiencies in this technique, such as the problem of too much noise caused by the rapid changes in the high gradient field of the EP sequence. Still, this deficiency can be solved by ultra-fast imaging and the development of noise reduction techniques.

Multi-shot echo-planar diffusion tensor imaging has been the focus of research in the early period of DTI imaging. This sequence of RF initiation only supplements the k-space region of the k-space region, and supplements it after multiple bit k-spaces. The tortured appearance of the graphics caused by the susceptibility artifacts and the lack of clearness in the graphics caused by T_2 * are significantly reduced because the echo chain is greatly reduced. So, we can use higher resolution imaging. However, in order to overcome the random phase shifts due to the physical activity in this sequence, we must develop techniques to reduce the activity artifacts. We use ECG control and breathing control to supplement the pulse and breathing disturbances. Currently, the most commonly used method is the navigation echo method [13]. This technology can see and continuously correct the phase changes in the k-space lines collected at multiple time points before and after the imaging. However, even with the above technology, the active artifacts are not eliminated. It will be completely eliminated, but the practical scope of the multiple-triggered planar echo technology is not very wide. Another important reason is that its imaging speed is very slow. And it cannot completely remove the graphic twisting caused by the magnetic susceptibility phenomenon.

Single-shot fast spin-echo diffusion tensor imaging (DTI). The above two types of EPI imaging sequences use EPI-based sequences in areas where the magnetic susceptibility is quite apparent, such as the brain stem. It is difficult to collect graphics with a high signal-to-noise ratio and normal inflexion, because the abovementioned two types of EPI imaging sequences are very sensitive to the non-uniformity of the magnetic field, so it easily causes the graphics to become curved. Therefore, we started to use some DTI imaging sequences that are not relat-

ed to the EPI class [14]. For example, with the FSE DTI sequence, its core is to add a pair of dispersion-sensitive gradients at both ends of the first clustering pulse of the HASTE sequence, and the signal collection is basically consistent with the HASTE sequence. It can get high-resolution and high signal-to-noise ratio images, and most of the susceptibility phenomena will not occur, because the phase compensation gradient and the focusing pulse are applied after the first echo collection [15]. However, the unclear images caused by the weakening of T_2 are the most serious problem of this sequence, and the short T_2 region is the most disturbed. The distance between the echoes before and after this technique is higher than the EPI sequence, because this technique requires that each echo must achieve a re-aggregation of the pulse, and the phase supplemental gradients must be added after collecting the samples. This will result in short T_2 region signals, and this causes a large amount of attenuation; so most of the echo signals in the future cannot be detected, resulting in unclear graphics. In addition, the precipitation of high RF energy in the HASTE sequence may cause an uncomfortable reaction in the subject's body. The temperature in some areas increases, disturbing the normal diffusion of the tissue and making the signal worse.

The morphology of knee bone inflammation and the MR measurements of the T_2 values are related to clinical research

Knee osteoarthritis is a chronic joint disease characterized by the degeneration, destruction, and bone hyperplasia of the articular cartilage. It is the most common cause of joint pain, morning stiffness, and dysfunction. There are no effective drugs that can completely cure OA [15]. One of the main problems limiting the improvement of OA treatment methods is that there is no accurate, non-invasive method for monitoring the progress of the articular cartilage. As a traditional OA examination method, plain film alone cannot directly observe or evaluate the cartilage changes, and the diagnosis of early OA is very limited. With the development of MIR imaging technology, the changes in MIR sensitivity to the articular cartilage can be accurately and reliably evaluated, so MIR enables us to better study and understand the very delicate, early abnormal articular cartilage before clinically and radiologically detecting the pre-disease conditions. Foreign studies have shown that the sensitivity of the 3.0T MR imaging system for cartilage damage is 66%-80%, and the specificity is 80%-97% [16]. Studies such as the Whole-Organ Magnetic Resonance Imaging Score (WORMS Lynch) and other studies have shown that WORMS is highly reliable in determining the occurrence of cartilage loss. MR T_2 mapping imaging is a quantitative analysis of articular cartilage done by measuring the T_2 lateral relaxation time changes in the internal tissue components to further diagnose early cartilage lesions, such as the degeneration of the OA cartilage in the knee joint. Due to changes in the water content and the destruction of the collagen network, the T_2 value increases compared to the T_2 value of normal knee cartilage.

At present, the results of the MR manifestations and the clinical correlations of knee joint OA cartilage defects are different at home and abroad. There is no correlation between the WOMAC score and cartilage thickness and the degree of cartilage defect. MRI shows a significant correlation between cartilage thickness and the width of the plain joint space ($P < 0.001$). Some Chinese scholars explored the diagnostic value of knee osteoarthritis using total knee magnetic resonance imaging scores and found that WORMS scores were positively correlated, indicating that the pain, stiffness, and function of knee OA patients can be explained using imaging, and a multiple linear regression analysis has confirmed this. The correlation between the knee joint OA cartilage Ta values and the clinical manifestations is still controversial.

This study first calculated the WORMS scores on the clinical manifestations of 10 healthy subjects and 70 knee OA patients before MR1 examinations of the knee joint and then applied 3.0T MRI conventional sequences, 3D-WATSC sequences, and T_2 mapping imaging to the healthy groups and the patients. The knees of the people in the group were scanned, the knee cartilage was WORMS scored, and the T_2 values were measured. According to the knee cartilage morphology WORMS scores, the knee OA patients were divided into the O1, O2, and O3 groups, and the knee joint OA cartilage WORMS and T_2 values were explored to see if

there was a correlation, and then we compared the differences between the T_2 values in the control group, the O1, O2, and O3 groups, and then we used MRI to semi-quantitatively and quantitatively analyze the knee OA to explore the correlation between the knee OA magnetic resonance manifestations and the clinical manifestations.

MRI evaluation

All the imaging data were evaluated by two experienced radiologists and a graduate student. On the Philips Extended MR Work skeletal inflammation 2.6.3.5 post-processing workstation, NII'R multi-planar reconstruction was used to reconstruct the sagittal 3D-WATSC sequence map to the knee coronal, sagittal, and transverse axis images. According to the revised Whole-Organ Magnetic Resonance Imaging Score (WORMS), the cartilage of the knee joint is divided into the medial region of femoral (MF, lateral region of femoral, LF, medial tibia), the medial region of the tibia (MT), the lateral region of tibia (LT, patella, P), and five subregions (see **Figure 1**) [16].

MRI assessment of cartilage morphology

We scored the cartilage morphology of each sub-region of the knee joint according to the WORMS semi-quantitative analysis 8-point scale using 0-6 points: 0 = normal; 1 = normal cartilage thickness but increased T2W1 signal; 2.0 = partial cartilage defect (maximum width < 1 cm); 2.5 = full-layer cartilage defect (maximum width < 1 cm); 3 = partial cartilage defect in multiple regions (2.0 points standard) spaced normal cartilage thickness zones or a 2-point standard with a maximum width greater than 1 cm but less than 75% of the subarea area; 4 = diffuse partial cartilage defect (greater than 75% of the subarea area); 5 = multiple layers full-layer cartilage defect (2.5 points standard), or a standard with 2.5 points, and width > 1 cm, but less than 75% of the subregional area; 6 = diffuse full-layer cartilage defect (75% of the subregional area), see **Figure 2** [4].

Included patients

70 patients with knee OA admitted to our hospital from March 2018 to March 2019 were recruited as the study cohort. The study was approved by the ethics committee of our hospital.

Inclusion criteria

Patients ≥ 60 years old, patients who met the relevant clinical diagnostic criteria for knee osteoarthritis, patients who completed the corresponding imaging examination, and patients who voluntarily signed the informed consent forms.

Exclusion criteria

Patients with primary malignant tumors, patients with systemic infections, And patients with a history of knee surgery.

Result

Clinical information

Among the 70 patients with knee OA, 39 were males and 31 were females, and they ranged in age from 60-79 years old, with an average age of (66.85±7.94) years. The 10 healthy subjects included 5 males and 5 females, ranging in age from 60-78 Years old, with an average age of (67.12±8.13) years old. There were no significant differences in the general clinical data between the two groups of subjects ($P > 0.05$).

Correlation between the T_2 values of the OA group and WORMS

T_2 mapping imaging has now been used clinically to assess knee cartilage tissue composition and ultrastructure. Various studies have confirmed that T_2 mapping can increase the detection rate of early cartilage degeneration in patients with knee OA and have found that degenerative changes occur earlier in the superficial layer of the cartilage, and the T_2 value of the cartilage gradually increases with age. T_2 mapping can also monitor the process of cartilage degeneration and cartilage repair after treatment. Some scholars have also used T_2 mapping imaging to quantitatively evaluate the transplanted cartilage of patients with matrix-induced autologous cartilage transplantation [16]. The follow-up periods were 3 months, 6 months, and 12 months. It was found that there were significant differences in the longitudinal changes of the deep and shallow T_2 values in the repair area. This study found that T_2 mapping can be used to evaluate the effect of articular cartilage repair after matrix-induced autologous cartilage transplantation. Observing the changes in the cartilage

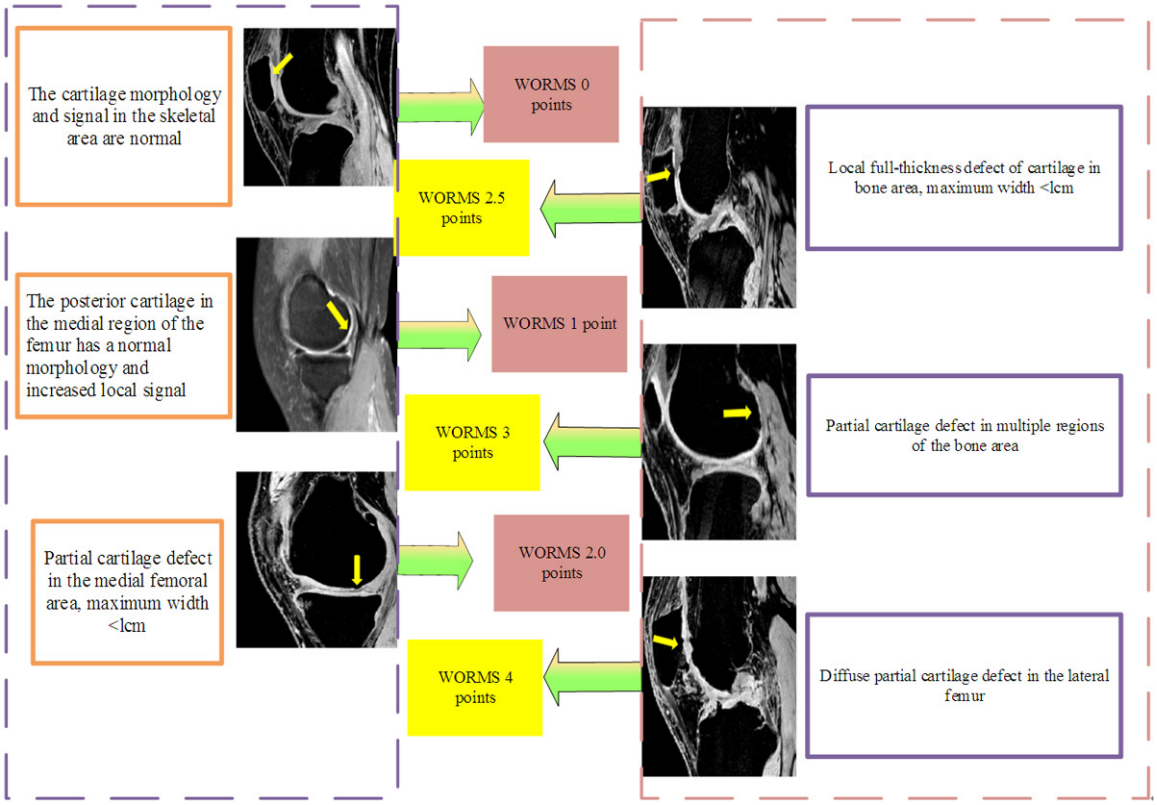

Figure 2. A WORMS semi-quantitative score diagram of articular cartilage morphology in OA patients. The normal cartilage morphology will also change by 1 point, 2-3 points represents focal cartilage changes, and 4-6 points represents full-thickness cartilage changes. According to the WORMS score of each subregion's cartilage, the subregion's cartilage was divided as follows: 0-1 into the mild (01) group, 2-3 into the moderate (02) group, and 4-6 into the severe (03) group, and the healthy control group was called the H group.

T_2 values in patients with and without loads after matrix-induced autologous chondrocyte transplantation, it was found that the differences in the T_2 values of multi-region cartilage were statistically significant, suggesting that using T_2 mapping imaging under load can provide more patient follow-up information about the cartilage repair tissue composition and the structure. In the knee cartilage T_2 value repeatability study, it was found that the cartilage T_2 value has a good consistency in the short-term and long-term repeatability measurements [17]. In the overall T_2 value measurement methods of each sub-region for setting multiple T_2 measurement methods of interest, the repeatability errors are small, as shown in **Figure 3**.

Correlation between the cartilage T_2 value and the WORMS in each OA group

A Pearson simple correlation analysis was used to evaluate the correlation between the cartilage T_2 values and the WORMS in each subarea of the OA group, and a correlation analysis chart was drawn. The specific analysis results are shown in **Table 1**. The analysis results show that the OA group skeletal areas, medial femur areas, and medial tibial areas, and that the correlation coefficients between the cartilage T_2 values and the WORMS in the lateral tibia were 0.66, 0.72, 0.71, and 0.85 ($P < 0.05$). The T_2 value in the lateral femur and the WORMS correlation coefficient were -0.03 ($P > 0.05$). This indicated that in the OA group, the cartilage T_2 values of the medial femoral, medial tibia, and lateral tibial areas were positively correlated with WORMS, and the T_2 values of the lateral femur were not related to WORMS, as shown in **Figure 4**.

Differences in the cartilage T_2 values between the subgroups

A univariate analysis of the variance comparing the differences between the T_2 values of each subregion among the groups showed that,

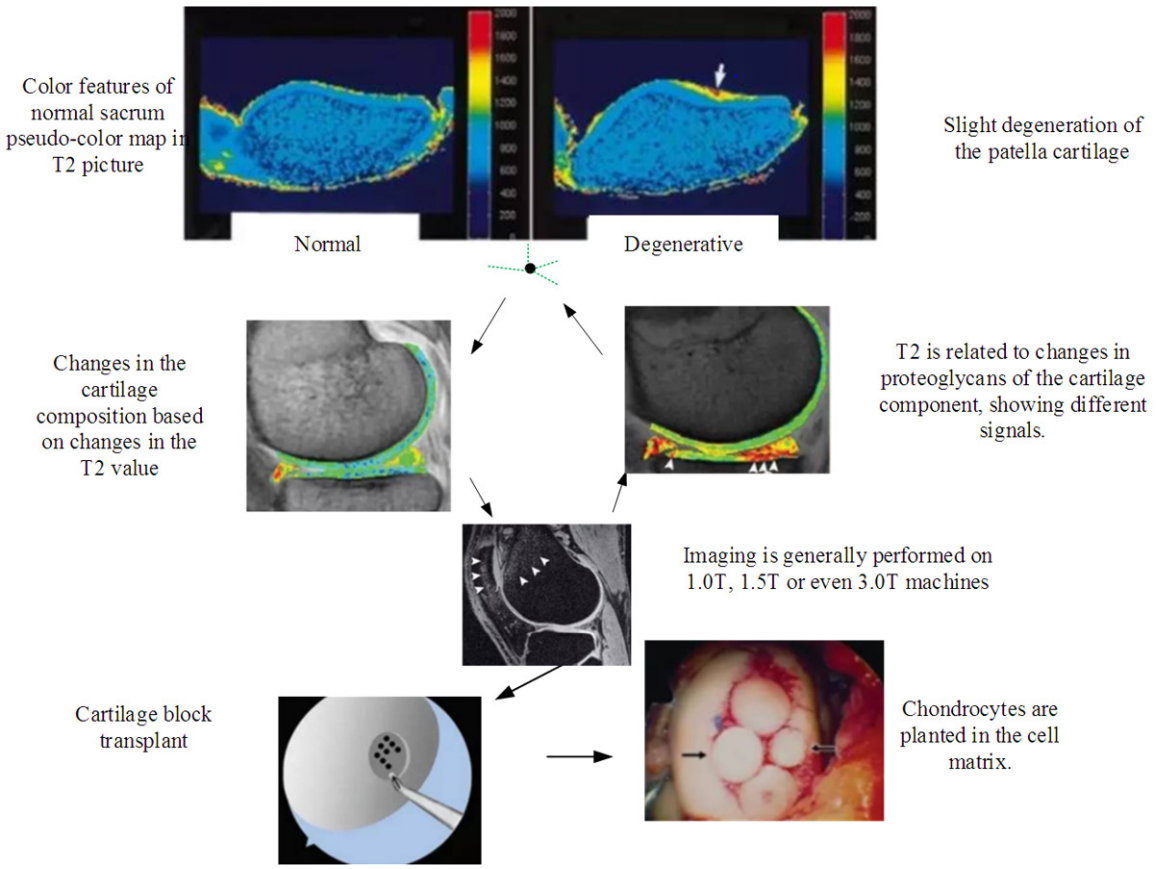

Figure 3. T_2 mapping imaging.

Table 1. Correlation analysis of the cartilage T_2 values and the WORMS in each subregion of the OA group

T_2 value	WORMS score	
	R	*P*-value
P	0.66	0.00
MF	0.72	0.00
LF	-0.03	0.73
MT	0.71	0.00
LT	0. 85	0.00

except for the T_2 values of the lateral femurs, there were no significant differences between the groups ($P > 0.05$), and the T_2 values of the other subregions in each group were different. The inequalities are equal ($P < 0.05$). The T_2 value of each sub-region gradually increases with an increase in the grade. The results show that, except for the T_2 values between the H group and the 01 group in the lateral region of the tibia, there were no significant differences in the T_2 values between the 01 group and the 02 group in the skeletal region ($P < 0.05$), and the differences in the other subregions were statistically significant between the groups, as shown in **Table 2** and **Figure 5**.

Since patients in the OI group have woRNIs scores of 0-1, the normal cartilage woRNIs scores can also be expressed as OI points. Based on the above results, the T_2 values between the H group and the 01 group were calculated for the bone, medial femoral, and medial tibial regions. The differences in the districts were analyzed using ROC curves to determine the diagnostic efficacy of the T_2 values. A statistical analysis was performed to obtain the ROC curve of the T_2 values in the skeletal, medial femur, and medial tibial regions in the H and 01 groups. The T_2 value of the best test performance of the bone regions in the H group and the 01 group was 34.25 ms using the Jordon index, the most approximate index was 0.87, the sensitivity was 78.23%, the specificity was 100%, and the area under the curve was 0.82. Using T_2 the best test performance of the medi-

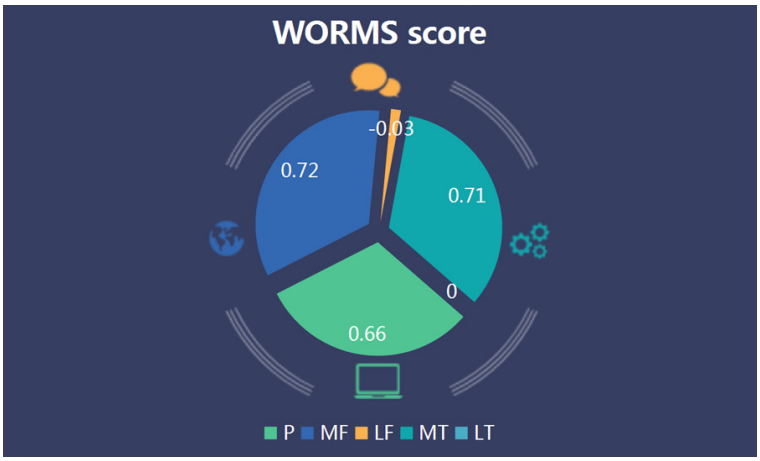

Figure 4. T_2 values of the cartilage in each subregion of the OA group.

al femoral region between the H and O1 groups was 45.21, the most approximate index was 0.47, the sensitivity was 67.38%, the specificity was 79%, and the area under the curve was 0.76. The medial tibia of the best test performance between the H group and the O1 group was 32.48 ms, the most approximate index was 0.38, the sensitivity was 44.73%, the specificity was 69%, and the area under the curve was 0.52 (see **Table 3** and **Figure 6**).

Discussion

Due to the innovative development of MRI software and hardware technology, MRI continues to show its potential in knee OA. Especially with the continuous extension of the human lifespan, the knees have become a major factor in reducing the quality of life and happiness index of middle-aged and elderly people. MRI only provides information on the morphology and volume integrity of articular cartilage, but it also evaluates the collagen and mucopolysaccharide changes in the cartilage. Foreign studies have shown that the sensitivity of the 3.0T MR imaging system for cartilage damage is 66%-80%, and the specificity is 80%-97%.

The correlation between the cartilage T_2 value and WORMS

Joseph et al. used a longitudinal study of cartilage T_2 values with cartilage degeneration in patients with OA, and, using a revised WORMS, divided the knee joint into five regions and calculated cartilage degeneration scores [13]. The results showed that as the WORMS score increased, the cartilage T_2 value also increased, confirming that there was a positive correlation between the T_2 value and the WORMS score. Chinese scholars increased the sample content and divided knee joint OA into mild, recombined, and normal classifications using MR, which showed statistically significant differences in the T_2 values between mild-severe OA and healthy-severe OA, which increased as the disease increased [13]. Moreover, the area with the most significant differences in the T_2 values is mainly in the load-bearing area, which reflects the gradual process of cartilage degeneration and supports the damage mechanism of knee OA cartilage [15]. T_2 mapping imaging of human articular cartilage in vitro was compared with the cartilage's histological grade using 3.0T MRI. The T_2 value differences between the grades were statistically significant, and the two were positively correlated ($P = 0.313$, $P < 0.05$), indicating the T_2 value. It is a better biological marker of OA cartilage and it is more suitable for the early diagnosis of knee OA [16].

In this study, the correlation between the T_2 values of each subarea in knee OA patients and the WORMS were compared. According to the WORMS grouping, the differences between the T_2 values of each subarea between the groups were compared. The results highlighted the OA group's skeletal area, medial femur area, and tibia. The T_2 values of the cartilage in the medial region and the lateral region of the tibia were positively correlated with the WORMS. The T_2 value of the cartilage in the lateral region of the femur had no correlation with the WORMS. The T_2 value of each subregion gradually increased with the increase of the grade. A pairwise comparison found that there was no significant difference in T_2 between the H and O1 groups in the lateral region of the tibia or between the O1 and O2 groups in the skeletal region. The differences in the other subregions were statistically significant between the two groups, indicating the T_2 value's ability to distinguish the severity of knee OA. And the T_2 value of the skeletal, medial femur, and medial tibia regions were sig-

Table 2. The average T_2 value of each subregion in each group

Group	P	MF	LF	MT	LT
Group H	32.19+1.24	42.18+1.83	42.48+1.27	31.28+1.92	30.24+2.14
O1 group	37.29+2.14	45.28+2.18	47.28+2.81	33.29+1.82	31.28+3.21
O2 group	40.24+4.85	48.29+3.91	47.20+3.81	38.48+1.30	37.96+2.95
O3 group	50.38+3.81	52.48+4.81	48.10+4.75	41.39+3.95	45.29+3.71
F	36.40	32.93	1.74	36.29	52.81
P	0.00	0.00	0.16	0.00	0.00

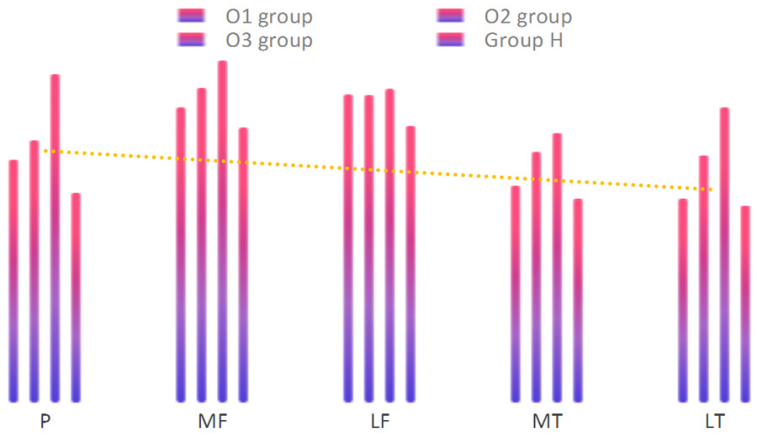

Figure 5. Average T_2 values by subregion.

Table 3. Evaluation of the T_2 values of the skeletal, the medial femoral, and the medial tibial regions in groups H and O1

Sub-area	Critical value (ms)	Maximum Jordon index	Area under the curve	Sensitivity (%)	Specificity (%)
Skeletal area	34.24	0.87	0.82	78.23	100
Medial femoral area	45.21	0.47	0.76	67.38	79
Medial tibial region	32.48	0.38	0.52	44.73	69

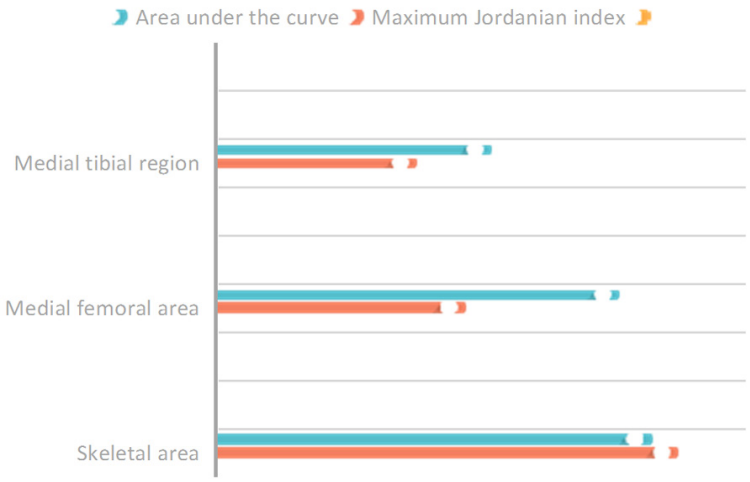

Figure 6. T_2 values of the skeletal, the medial femoral, and the medial tibial regions in the H and O1 groups.

nificantly different between group H and O1. The sensitivities of the T_2 value to diagnose early OA of the knee joint were 78.3%, 68.2%, and 54.8%, respectively. The degrees are 100%, 80%, and 70%, indicating that the areas with the greatest difference in T_2 values are mainly in the knee bearing area. The T_2 value enables an early diagnosis of knee OA and can detect lesions before the cartilage morphology changes. As reported by other scholars, the soft tissue inflammation in patients with knee OA can be observed using MRI examination, thus correlating with the patient's clinical symptoms [20, 21].

Innovations and limitations of the study

When comparing the differences in the cartilage T_2 values between groups, this study grouped the degree of OA cartilage damage in each sub-area according to the WORMS in each sub-area, and then compared the differences in the T_2 values in each sub-area between the groups. An error of comparison of the T_2 value differences caused by the grouping of the total cartilage damage of the knee joint was introduced. Furthermore, the diagnostic efficacy of the T_2 values in the cartilage, medial femur, and medial tibial areas with significant differences in the cartilage T_2 values between

the healthy group and the mild OA group was further analyzed.

Conclusion

In order to clarify the correlation between the imaging manifestations and the clinical manifestations of OA cartilage injuries, it is necessary to exclude the influence of the irrelevant factors and to explore the predictive effect of the MRI manifestations on the early symptoms of OA. Helminth is a semi quantitative MRI evaluation index, and it can effectively evaluate the changes in the knee joint OA cartilage and reflect patients' clinical manifestations to a certain extent. The T_2 value of the MRI quantitative evaluation index can distinguish the injury degree of OA cartilage of the knee joint, find the change in the cartilage morphology before the lesion, and explain its clinical manifestations.

There are also some shortcomings in this study: the subjective scores of the cartilage WORMS, the random measurement errors of the T_2 values using the manual calibration method, the T_2 imaging takes a long time, some patients cannot tolerate some images, and motion artifacts may appear. In the correlation analysis of the T_2 values of the cartilage and WORMS scores, synovitis related to OA, meniscus injury, ligament injury, joint effusion, or bone marrow cannot be completely excluded, nor can the effect of edema on the clinical symptoms.

Disclosure of conflict of interest

None.

Address correspondence to: Guangbin Wang, Department of Medical Imaging, Yiyuan People's Hospital, No. 21 Shengli Road, Yiyuan County, Zibo City, Shandong Province China; Tel: +86-021-13806408986; E-mail: wangguanbin113@126.com

References

[1] Barsotti S, Zampa V, Talarico R, Minichilli F, Ortori S, Iacopetti V, D'ascanio A, Tavoni AG, Bombardieri S, Mosca M and Neri R. Thigh magnetic resonance imaging for the evaluation of disease activity in patients with idiopathic inflammatory myopathies followed in a single center. Muscle Nerve 2016; 54: 666-672.

[2] Alfuraih AM, O'Connor P, Tan AL, Hensor EMA, Ladas A, Emery P and Wakefield RJ. Muscle shear wave elastography in idiopathic inflammatory myopathies: a case-control study with MRI correlation. Skeletal Radiol 2019; 48: 1209-1219.

[3] Ran J, Ji S, Morelli JN, Wu G and Li X. T2 mapping in dermatomyositis/polymyositis and correlation with clinical parameters. Clin Radiol 2018; 73: 1057-1113.

[4] Lee K, Shin Y, Huh J, Sung YS, Lee IS, Yoon KH and Kim KW. Recent issues on body composition imaging for sarcopenia evaluation. Korean J Radiol 2019; 20: 205-217.

[5] Kubínová K, Dejthevaporn R, Mann H, Machado PM and Vencovský J. The role of imaging in evaluating patients with idiopathic inflammatory myopathies. Clin Exp Rheumatol 2018; 114: 74-81.

[6] Yin L, Xie ZY, Xu HY, Zheng SS, Wang ZX, Xiao JX and Yuan Y. T2 Mapping and fat quantification of thigh muscles in children with Duchenne muscular dystrophy. Curr Med Sci 2019; 39: 138-145.

[7] Guimaraes JB, Zanoteli E, Link TM, de Camargo LV, Facchetti L, Nardo L and Fernandes ADRC. Sporadic inclusion body myositis: MRI findings and correlation with clinical and functional parameters. AJR Am J Roentgenol 2017; 209: 1340-1347.

[8] Eller-Vainicher C, Falchetti A, Gennari L, Cairoli E, Bertoldo F, Vescini F, Scillitani A and Chiodini I. Diagnosis of endocrine disease: evaluation of bone fragility in endocrine disorders. Eur J Endocrinol 2019; 180: 213-232.

[9] Chawla A, Dubey N, Chew KM, Singh D, Gaikwad V and Peh WC. Magnetic resonance imaging of painful swollen legs in the emergency department: a pictorial essay. Emerg Radiol 2017; 24: 577-584.

[10] Pinal-Fernandez I, Casal-Dominguez M, Carrino JA, Lahouti AH, Basharat P, Albayda J, Paik JJ, Ahlawat S, Danoff SK, Lloyd TE, Mammen AL and Christopher-Stine L. Thigh muscle MRI in immune-mediated necrotising myopathy: extensive oedema, early muscle damage and role of anti-SRP autoantibodies as a marker of severity. Ann Rheum Dis 2017; 76: 681-687.

[11] Brockway JP. Two functional magnetic resonance imaging f(MRI) tasks that may replace the gold standard, Wada testing, for language lateralization while giving additional localization information. Brain Cogn 2000; 43: 57-59.

[12] Bray TJP, Bainbridge A, Punwani S, Ioannou Y and Hall-Craggs MA. Simultaneous quantification of bone edema/adiposity and structure in inflamed bone using chemical shift-encoded MRI in spondyloarthritis. Magn Reson Med 2018; 79: 1031-1042.

[13] Guimarães JB, Nico MA, Omond AG, Aivazoglou LU, Jorge RB, Zanoteli E and Fernandes ARC.

Diagnostic imaging of inflammatory myopathies: new concepts and a radiological approach. Curr Rheumatol Rep 2019; 21: 8.
[14] Kubínová K, Mann H and Vencovský J. MRI scoring methods used in evaluation of muscle involvement in patients with idiopathic inflammatory myopathies. Curr Opin Rheumatol 2017; 29: 623-631.
[15] Beltran LS, Samim M, Gyftopoulos S, Bruno MT and Petchprapa CN. Does the addition of DWI to fluid-sensitive conventional MRI of the sacroiliac joints improve the diagnosis of sacroiliitis? AJR Am J Roentgenol 2018; 210: 1309-1316.
[16] Schmidt S, Hafner P, Klein A, Rubino-Nacht D, Gocheva V, Schroeder J, Naduvilekoot Devasia A, Zuesli S, Bernert G, Laugel V, Bloetzer C, Steinlin M, Capone A, Gloor M, Tobler P, Haas T, Bieri O, Zumbrunn T, Fischer D and Bonati U. Timed function tests, motor function measure, and quantitative thigh muscle MRI in ambulant children with Duchenne muscular dystrophy: a cross-sectional analysis. Neuromuscul Disord 2018; 28: 16-23.
[17] Rozenberg D, Martelli V, Vieira L, Orchanian-Cheff A, Keshwani N, Singer LG and Mathur S. Utilization of non-invasive imaging tools for assessment of peripheral skeletal muscle size and composition in chronic lung disease: a systematic review. Respir Med 2017; 131: 125-134.
[18] Thøgersen KF, Simonsen JA, Hvidsten S, Gerke O, Jacobsen S, Høilund-Carlsen PF, Buch-Olsen KM and Diederichsen LP. Quantitative 3D scintigraphy shows increased muscular uptake of pyrophosphate in idiopathic inflammatory myopathy. EJNMMI Res 2017; 7: 97-101.
[19] Tiwari V, Gamanagatti S, Mittal R, Nag H and Khan SA. Correlation between MRI and hip arthroscopy in children with Legg-Calve-Perthes disease. Musculoskelet Surg 2018; 102: 153-157.
[20] Zhao X, Ruan J, Tang H, Li J, Shi Y, Li M, Li S, Xu C, Lu Q and Dai C. Multi-compositional MRI evaluation of repair cartilage in knee osteoarthritis with treatment of allogeneic human adipose-derived mesenchymal progenitor cells. Stem Cell Res Ther 2019; 10: 308-311.
[21] Liu J, Chen L, Tu Y, Chen X, Hu K, Tu Y, Lin M, Xie G, Chen S, Huang J, Liu W, Wu J, Xiao T, Wilson G, Lang C, Park J, Tao J and Kong J. Different exercise modalities relieve pain syndrome in patients with knee osteoarthritis and modulate the dorsolateral prefrontal cortex: a multiple mode MRI study. Brain Behav Immun 2019; 82: 253-263.